J. Fluid Mech. (1984), *vol.* 143, *pp.* 413–427
Printed in Great Britain

Organized structures in a reattaching separated flow field

By T. R. TROUTT, B. SCHEELKE AND T. R. NORMAN

Department of Mechanical Engineering, Washington State University,
Pullman, WA 99164-2920

(Received 7 September 1983 and in revised form 28 February 1984)

Spanwise structures in a two-dimensional reattaching separated flow were studied using multisensor hot-wire anemometry techniques. The results of these measurements strongly support the existence and importance of large-scale vortices in both the separated and reattached regions of this flow. Upstream of reattachment, vortex pairings are indicated and the spanwise structures attain correlation scales closely comparable to previously measured mixing-layer vortices. These large-scale vortices retain their organization far downstream of the reattachment region. However, pairing interactions appear to be strongly inhibited in this region. It is suggested that large-scale vortex dynamics are primarily responsible for some of the important time-averaged features of this flow. Notably, the reduction of turbulence energy in the reattachment region and the slow transition of the mean flow downstream of reattachment are attributed to effects associated with these vortices.

1. Introduction

Over the past decade considerable research efforts have been expended concerning the subject of orderly structures in turbulent flow fields. For reasons of simplicity, most of these efforts have concentrated on self-preserving flows of relatively simple geometry such as the plane mixing layer and the plane boundary layer. The primary structures in these flows, however, seem to be dependent on the mean-flow geometry and the location of solid-surface constraints. For example, large-scale spanwise vortices appear to dominate the dynamics of the plane mixing layer (Brown & Roshko 1974; Browand & Troutt 1980*a*). On the other hand, the dominant structure of the plane boundary layer may be a vortex with a hairpin or horseshoe shape (Perry & Chang 1982).

Several questions have, of course, been raised about these somewhat subjective structures. One question has been directed towards their existence in flows with more complex boundary or mean-flow conditions. Another question involves the practical importance of these structures with respect to time-average flow properties, since the structures appear randomly in space and time.

The present study is primarily concerned with the identification of organized structures in a flow field of somewhat more mean-flow complexity than the plane flows previously mentioned. The flow field is produced by the motion of a turbulent boundary layer over a two-dimensional downstream-facing step. Since the step height is large compared with the upstream boundary-layer thickness, the flow field immediately downstream of the step may be thought of as a boundary layer in transition to a free mixing layer. Several step heights farther downstream, because of the mixing-layer growth, the flow begins to be influenced by the wall again, and thus starts the transition back to a bounded flow.

This flow field exhibits a number of unusual mean-property variations in the downstream direction. Probably two of the most interesting and important are the abrupt decline in Reynolds stresses and turbulence energy near the reattachment region, and, secondly, the extremely slow downstream adjustment of the reattached mean-velocity profiles to conventional turbulent boundary-layer profiles (see e.g. Chandrsuda & Bradshaw 1981). Although our experimental study was not explicitly directed towards these mean-flow features, we believe our results may give some insight into their possible causes.

The motivation behind the experimental approach used in the present study can be attributed to the experiments conducted by Browand & Troutt (1980*a*) on the plane mixing layer. In that study, a line of hot wires was positioned across the span of a mixing layer at a vertical position just outside the turbulent-flow interface. This vertical position was chosen to optimize the influence of large-scale structures on the sensor signals. The instantaneous velocity signals from these sensors were then used to examine the nature of large-scale spanwise vortices within the mixing layer. Browand & Troutt's results demonstrated that a large-scale quasi-two-dimensional structure was an inherent part of the asymptotic mixing layer. This structure was later found by Browand & Troutt (1980*b*) to be apparent in mixing layers over a wide range of velocity ratios with both laminar and turbulent boundary-layer input conditions.

The specific objectives of the present research were to determine the degree and development of spanwise organization in the step flow and to evaluate the importance of these structures in the overall flow-field development. To analyse these structures experimentally, the multisensor techniques used by Browand & Troutt (1980*a*) were employed.

2. Experimental apparatus and flow conditions

The experiments were conducted using an open-circuit wind tunnel driven by an inlet blower. The blower is connected to the wind tunnel through a section of flexible walls to reduce fan-vibration effects. Downstream of the inlet, an expanded area section containing straws and fine screens is used to produce a uniform flow. A contraction section of area ratio 7 connects the tunnel to removable test sections. Figure 1 shows a schematic of the test section used in this study. The section dimensions are 240 cm in the downstream (x) direction, 61 cm in the vertical (y) direction and 91 cm in the spanwise (z) direction. A 5.6 cm high raised step was placed on the bottom floor of the test facility. The upstream transition from the facility floor to the step was made using a cubic contour. The raised step section was 46 cm in length from the end of the upstream transition to the step edge. All working surfaces in the test facility were constructed from Plexiglas.

The measurements reported here were obtained using single-sensor hot wires with their wires aligned in the z-direction. The anemometers used were Thermal Systems Inc. model 1053B bridges driven by 1051-6 power supplies. The high-end frequency response of these anemometer systems is approximately 10 kHz.

Data acquisition was accomplished using a 16 bit microcomputer system. This system is capable of accepting up to 16 channels of data input at an overall sampling rate of 125 kHz. A maximum of 10 channels of simultaneously acquired hot-wire data are reported here. The digitization rates employed ranged from 8 kHz per channel

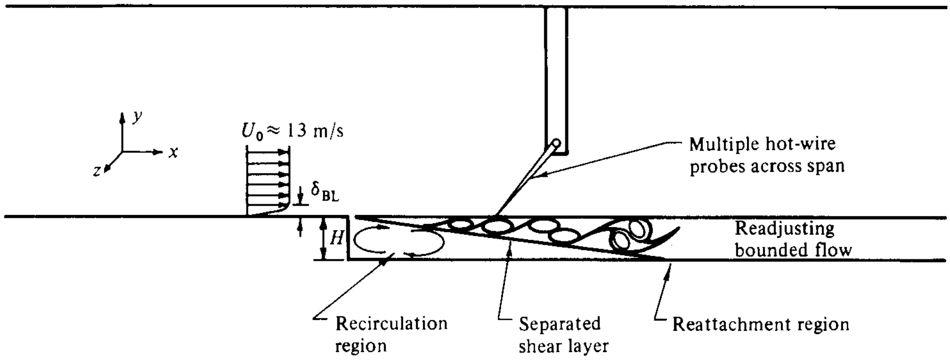

FIGURE 1. Schematic of experimental arrangement.

at positions close to the step to 4 kHz per channel for positions farther downstream. The digitized amplitudes were acquired with 12 bit resolution. Data analyses were performed primarily on a Prime 400 minicomputer.

Mean-velocity measurements from downstream of the step were measured with a Pitot-static pressure probe. The probe was turned downstream in the reverse-flow region. Turbulence-intensity measurements reported for levels below 35% were obtained using calibrated single-sensor hot-wire probes. For the multisensor results obtained on the upper edge of the turbulent flow non-calibrated hot wires were used since the fluctuating voltage can be assumed to be proportional to the fluctuating velocity at low amplitudes.

The measurements reported here were all conducted with a nominal free-stream velocity of 13 m/s prior to the step edge. Free-stream turbulence intensity levels were approximately 0.6%. The free-stream mean-velocity variation in the spanwise dimension was within ± 2% over the measurement region. The momentum thickness of the boundary layer at the step edge was 0.10 cm. The ratio of this boundary-layer momentum thickness to the step height is approximately 0.018. The momentum-thickness Reynolds number of the boundary layer at this position is 920. The Reynolds number of this step flow based on step height and free-stream velocity was 45000.

3.1. *Results – mean flow*

The boundary layer immediately upstream of the step edge was found to be in a turbulent state. Figure 2 shows the mean-velocity distribution of the boundary layer at $x/H = -1$ measured with a calibrated hot wire. The mean velocity is plotted as a logarithmic function of the non-dimensional vertical coordinate yu^*/ν, where u^* is the friction velocity and ν is the kinematic viscosity. The data follow closely the universal logarithmic curve, with a value of $u^* = 0.66$ m/s giving the best fit.

Longitudinal turbulence intensity levels measured across the boundary layer are shown in figure 3. The turbulence-intensity levels and their vertical distribution measured here compare well with similar measurements by other investigators (Klebanoff 1955; Browand & Latigo 1979).

Mean-velocity profiles measured by a Pitot-static pressure probe downstream of the step are shown in figure 4. Comparisons with Chandrsuda & Bradshaw (1981) are shown for $x/H = 3.4$ and 4.4. The slight differences observed between this flow and Chandrsuda & Bradshaw's can probably be attributed to differences in initial conditions (Chandrsuda & Bradshaw's flow had a laminar-boundary-layer initial

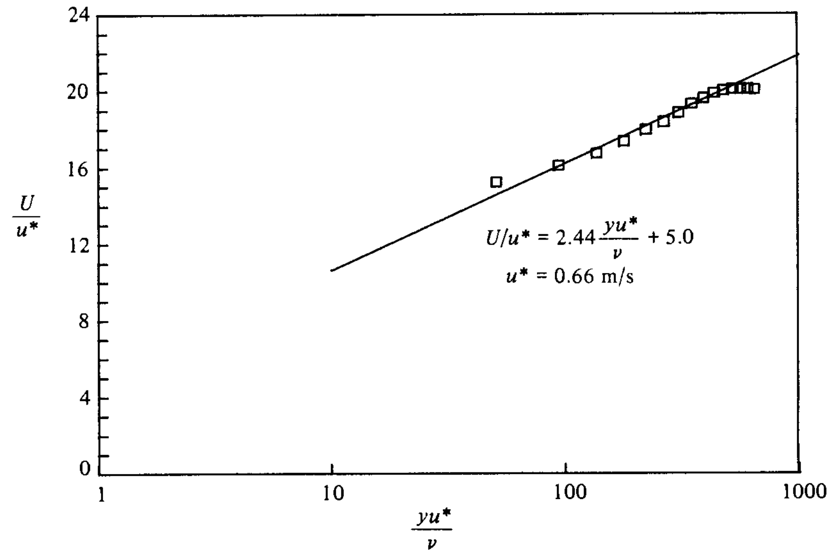

FIGURE 2. Mean-velocity distribution of boundary layer at $x/H = -1$ plotted as a logarithmic function of vertical coordinate.

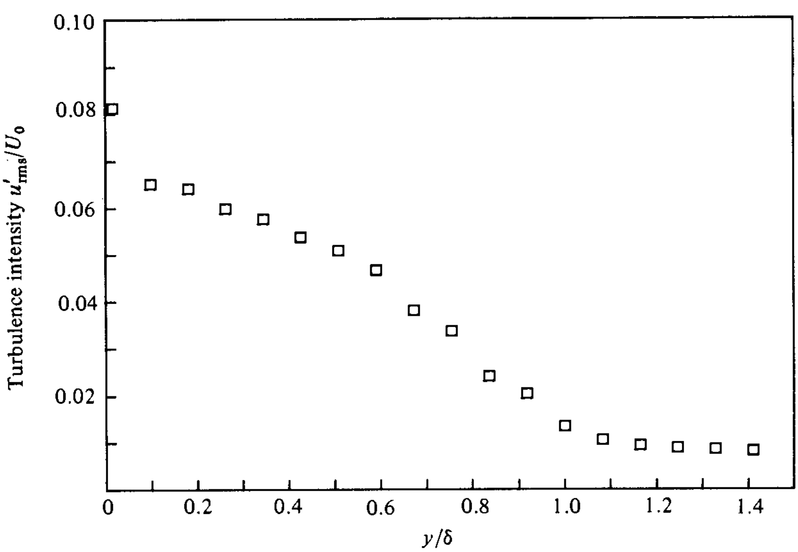

FIGURE 3. Longitudinal turbulence intensity across boundary layer at $x/H = -1$.

condition), and to slight differences in the external pressure fields of the two flows. The mean-velocity profiles indicate a reattachment region near $x/H = 7$. This reattachment length is the expected distance for a step flow at high Reynolds number with a negligible external pressure gradient (Kuehn 1980). The mean velocity profiles downstream of the reattachment area show a persistent region of retarded fluid in the outer portion of the boundary layer. This dip in the downstream velocity profiles has been noted in other studies of the step flow (Chandrsuda & Bradshaw 1981).

The downstream development of the maximum slope thickness δ_ω for the separated shear layer prior to reattachment is shown in figure 5. The maximum slope thickness

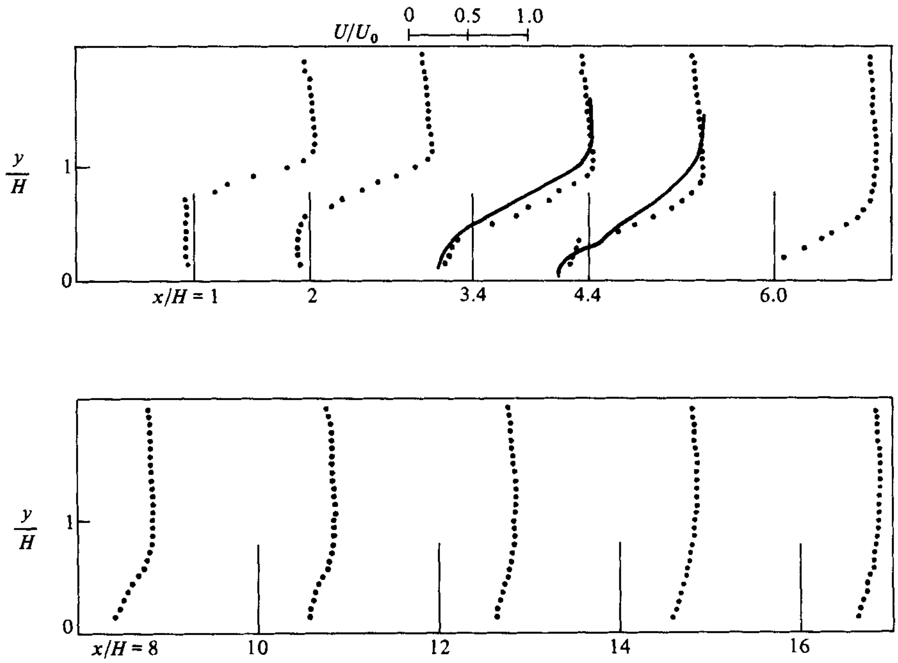

FIGURE 4. Mean-velocity profiles from downstream of step: ●, present measurements; ——, from Chandrsuda & Bradshaw (1981).

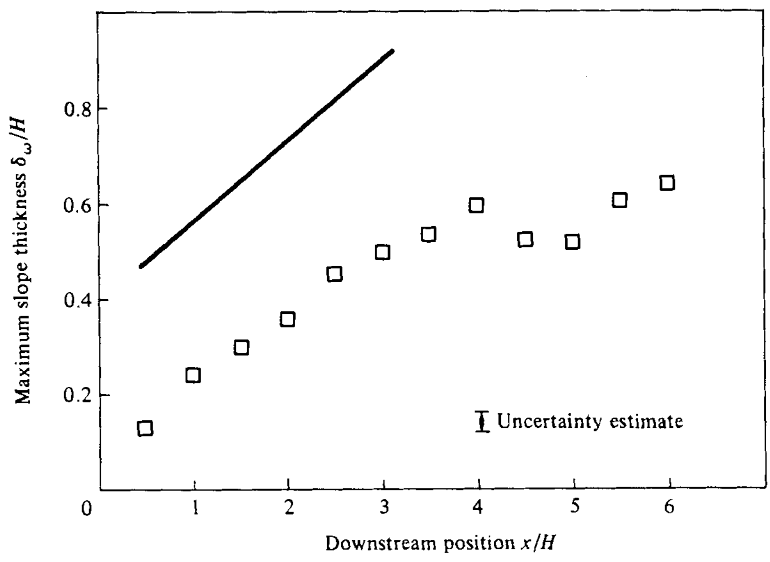

FIGURE 5. Downstream development of maximum slope thickness δ_ω for separated flow upstream of reattachment: □, step-flow measurements; ——, expected $\lambda = 1$ mixing-layer growth rate.

is a measure commonly used for two-stream mixing-layer studies. To calculate its value for the step flow, the slower-speed stream of the analogous mixing layer was assumed to have a zero velocity. This assumption gives a value for the velocity-ratio parameter used in the two-stream studies of $\lambda = (U_H - U_L)/U_H + U_L) = 1.0$. Here U_H represents the free-stream velocity on the high-speed side of the mixing layer and

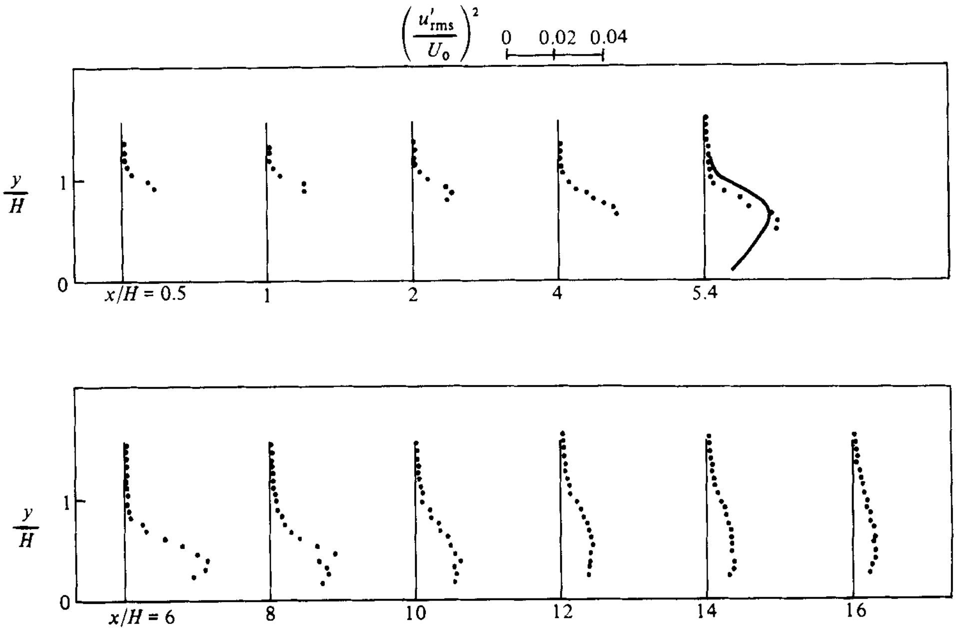

FIGURE 6. Longitudinal fluctuation energy profiles from downstream of step: ●, present measurements; ——, from Chandrsuda & Bradshaw (1981).

U_L the free-stream velocity on the low-speed side. The expected slope for the growth of a fully developed $\lambda = 1.0$ mixing layer is shown on the figure ($d\delta_\omega/dx = 0.17$).

Between $x/H = 0.5$ and $x/H = 4.0$, δ_ω increases at what appears to be a linear rate. Beyond $x/H = 4.0$ mean-flow curvature effects and the solid surface constraint combine to abruptly halt the growth in δ_ω. A least-squares fit to the step-flow data between $x/H = 0.5$ and $x/H = 4.0$ gives a slope of 0.13 ± 0.018, which is reasonably close to the expected $\lambda = 1.0$ mixing-layer value.

Several hypotheses for the slight difference between the measured initial step-flow growth rate and the expected mixing-layer slope can be given. One obvious possibility is that the local value of λ for the step flow changes with downstream position (λ varies from 1.0 to 1.6 in the region prior to reattachment). This explanation, however, would imply that a higher growth rate than 0.17 should be expected. The measurements clearly do not support this.

A more likely explanation could be based on the observation by Browand & Latigo (1979) that a mixing layer originating from a turbulent boundary layer grows at a significantly slower rate for a considerable downstream distance. The reasons for this reduced growth rate are not well understood, but it may be attributed to a slight interference in vortex pairing caused by residual small-scale boundary-layer turbulence.

Profiles of the longitudinal fluctuation energy are presented in figure 6. Since these measurements were performed with a single-sensor hot wire, the reported data are limited to local turbulence intensities below 35%. A comparison with measurements by Chandrsuda & Bradshaw (1981) is shown at $x/H = 5.4$. Chandrsuda & Bradshaw's results were obtained with a cross-wire probe. The comparison between the two flows is reasonably close considering the complexity of the flow development and the inaccuracies involved in measuring high turbulence levels.

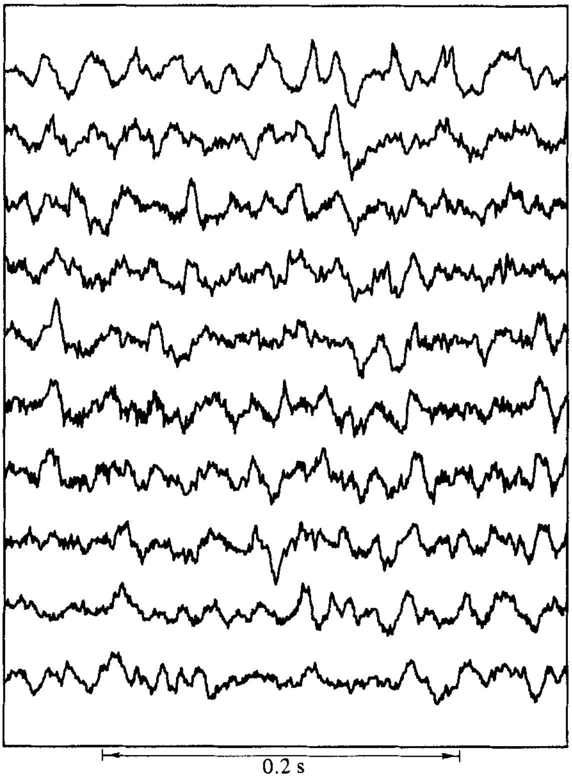

FIGURE 7. Typical velocity time traces from hot-wire array near turbulent-flow interface at $x/H = 6.0$, $u'_{rms}/U = 2\text{–}3\%$.

The reduction in turbulence energy by a factor of almost 2 between $x/H = 6$ and $x/H = 10$ is closely comparable to the decreases observed by Chandrsuda & Bradshaw (1981) in this region.

3.2. *Results – spanwise structures*

The simultaneous voltage outputs from ten hot wires displaced along the spanwise dimension are shown in figure 7 for the downstream position $x/H = 6$. The hot wires are positioned vertically just above the turbulent-flow interface at a turbulence-intensity level of approximately 2–3%. The probes are separated over a total spanwise distance of $6.5H$.

The signals show amplitude peaks which occur regularly in time and approximately simultaneously at numerous sensor locations. These features indicate that a significant level of spanwise organization is present in the separated flow at this downstream location. These signals are quite similar in appearance to the time traces reported by Browand & Troutt (1980*a*) from their asymptotic mixing-layer study. However, somewhat more high-frequency noise is apparent on these signals than those from Browand & Troutt. This difference is due to the higher levels of free-stream turbulence in this facility (0.6% compared to 0.3% for the mixing-layer facility). Following their interpretations, the regular oscillations in the time signals are indicative of the passage of large-scale vortex structures in the underlying turbulent flow.

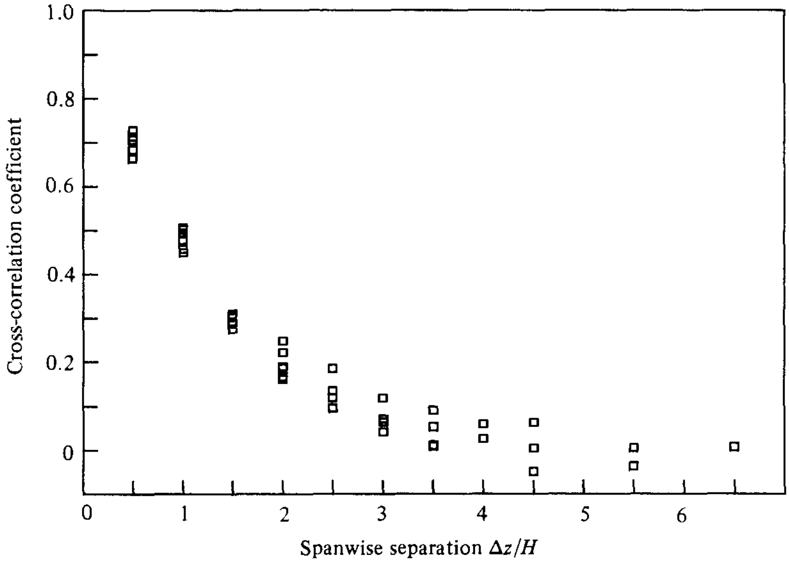

FIGURE 8. Zero-time-delay cross-correlation coefficient for all combinations of spanwise sensor displacements; $x/H = 6.0$.

As mentioned previously, the vertical positioning of the sensor array was chosen to optimize the effect of the large-scale structures on the sensor signals. Farther away from the turbulence interface the induced signals from the organized structures are too small with respect to the background turbulence in the free stream. At positions of higher turbulence intensity inside the shear layer, high-frequency effects obscure the large-scale organization. A more elaborate discussion of the effect of the vertical position is presented in Browand & Troutt (1983). All measurements on spanwise structure from various downstream locations to be reported here are from vertical positions of equivalent turbulent intensity (2–3 %).

To document quantitatively the development of spanwise correlation in this flow, the zero-time-delay cross-correlation coefficient between all spanwise sensor pairs was computed. Figure 8 shows the result for the downstream location of $x/H = 6$. The spread for different sensor pairs with the same spanwise displacement gives an indication of the errors involved in the measurement.

The downstream development of the spanwise correlation coefficient for fixed separations of $\Delta z/H = 0.5$, 1.0 and 1.5 are shown in figure 9. Each data point represents an average over several sensor pairs of equal displacement. The results show that rapid increases in spanwise correlation are produced by the separated shear layer prior to the reattachment region. This result indicates that large-scale mixing-layer-type vortices are prominent in the separated flow field. Near the reattachment region, the correlation values start to decline and reach a local minimum. This local minimum may be associated with a complex interaction between the recirculation region, the solid surface and the large-scale vortices.

Downstream of the local minimum associated with the reattachment region, the correlation values at the closest spacing of $\Delta z/H = 0.5$ show a gradual but steady decline. The correlation values for the largest sensor displacement, however, show a slight increase in correlation with downstream position in this region. This somewhat surprising result seems to indicate that the surface interaction with the

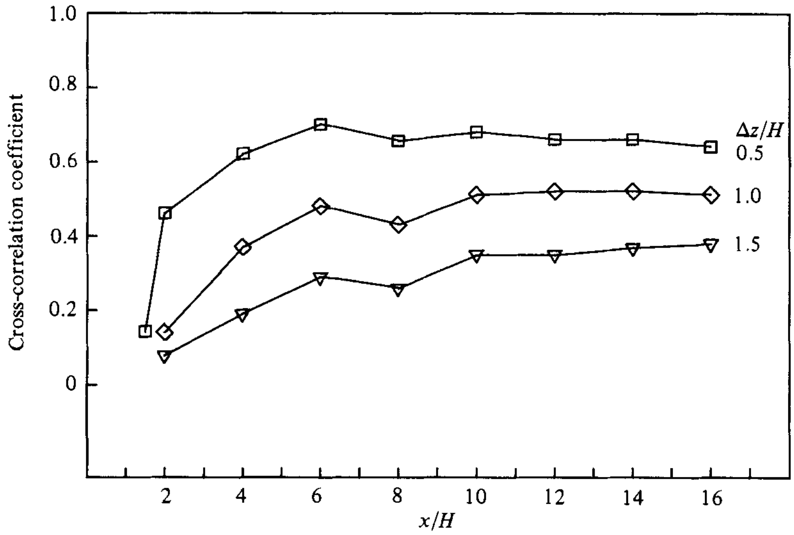

FIGURE 9. Downstream development of spanwise correlation coefficient for fixed spanwise separations: □, $\Delta z/H = 0.5$; ◇, 1.0; ▽, 1.5.

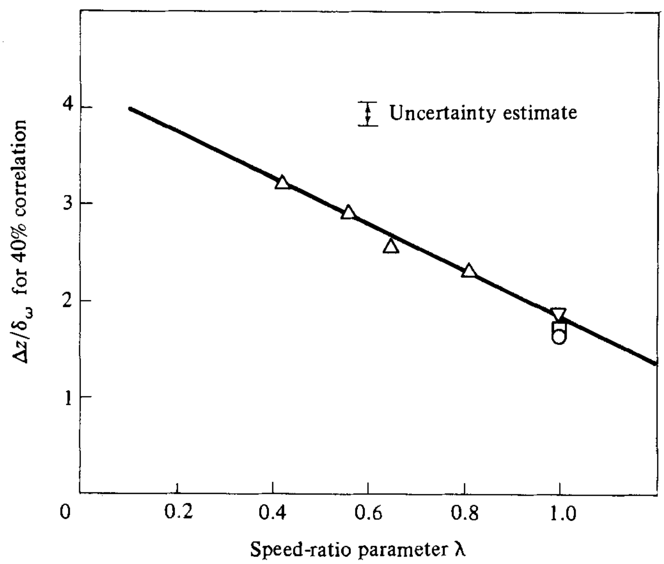

FIGURE 10. Normalized spanwise separation for 40% cross-correlation; comparison between asymptotic mixing-layer results from Browand & Trout (1983) and step-flow results: △, asymptotic mixing-layer results; □, step flow, $x/H = 2.0$; ○, step flow, $x/H = 4.0$; ▽, step flow, $x/H = 6.0$.

structures is causing them to acquire more irregularity at small scales while enhancing their global organization. This interesting result is discussed further in the Conclusion section.

To compare the spanwise scales prior to reattachment with the mixing-layer structures measured by Browand & Troutt (1980*b*), a plot of the separation distance associated with 40% correlation is given in figure 10 For both mixing-layer and step-flow results. The vertical axis on this plot gives the spanwise separation from the measurement location for 40% correlation, non-dimensionalized by the local

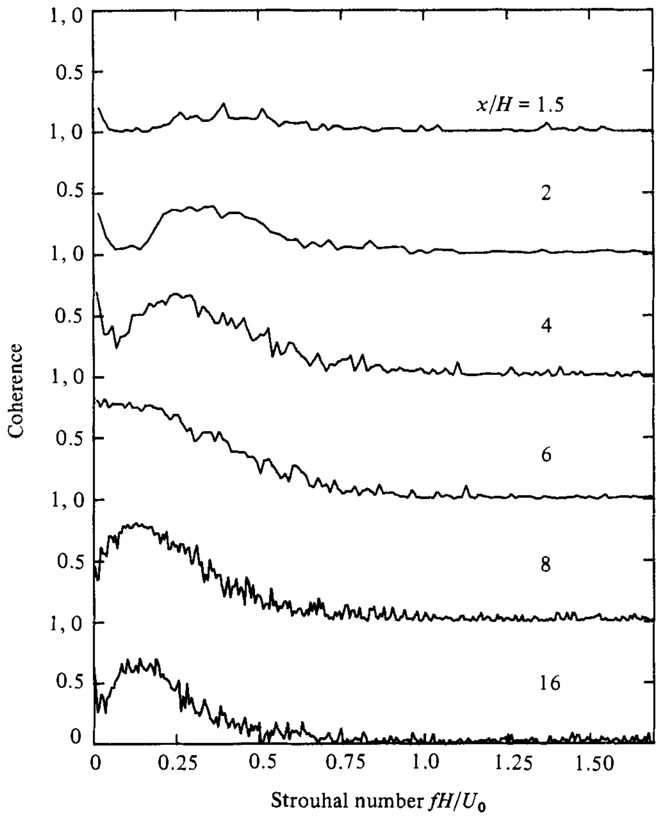

FIGURE 11. Coherence function between hot wires displaced $\Delta z/H = 0.5$ for several downstream locations.

maximum slope thickness δ_ω. The horizontal axis shows the value of λ for the various mixing-layer experiments. The spanwise correlation values for the mixing-layer results were measured at asymptotic downstream positions. Step-flow results from $x/H = 2$, 4 and 6 are shown on the figure. Although the local λ-values for these positions vary considerably, a value of $\lambda = 1$ was chosen for consistency with the mean-flow interpretations. All three step-flow correlation scales fall, within experimental error, on the line extrapolated from the mixing-layer experiments. These results demonstrate that organized structures with spanwise scales comparable to mixing-layer structures develop quickly in the separated flow.

The precise value of λ to be used for the step-flow results is somewhat debatable. Local values of λ significantly above 1 are found at $x/H = 2$ and 4. However, the initial δ_ω growth rate indicates a somewhat lower value of λ. A choice of $\lambda = 1$ seems to be a reasonable compromise for this situation.

Information concerning the spectral distribution of the spanwise coherence is shown in figure 11. These plots display the coherence function between two wires of constant separation $\Delta z/H = 0.5$ for downstream locations from $x/H = 1.5$ to $x/H = 16$.

At $x/H = 1.5$ two regions of significant coherence amplitude are noticeable. One region around $St = 0.25$–0.65 is most probably associated with the vortices created in the shear layer. The other region of non-negligible coherence is at the lowest resolvable frequencies of the measurement. These low frequencies may be associated with an overall unsteadiness of the entire recirculation region. Immediately downstream of $x/H = 1.5$ the coherence of the higher-frequency region grows rapidly in amplitude and shifts to lower frequencies. This shift to lower frequencies indicates that the initial vortices formed in the separated flow are pairing in agreement with the model of mixing-layer growth described by Winant & Browand (1974). The growth in the coherence amplitude implies that the spanwise scales of these vortices are also increasing in agreement with Browand & Troutt's (1980*a*) mixing-layer experiments.

The amplitude of the coherence function at the lowest frequencies also increases, and by $x/H = 6$ near reattachment no separation in the two regions is apparent. This result indicates that the coherence at the lowest frequencies in the upstream plots, which was attributed to an overall unsteadiness in the recirculation region, may be associated with the passage of large-scale vortices through the reattachment region. This possibility, however, remains conjectural at this point. In agreement with the cross-correlation measurements for $\Delta z/H = 0.5$, the coherence reaches its maximum amplitude (approximately 80%) at $x/H = 6$.

A direct comparison of the frequency content of the plots prior to reattachment with mixing-layer values can be made using local parameters for scaling the horizontal axis. For this comparison, the maximum slope thickness δ_ω and an average free-stream velocity $\frac{1}{2}(U_H + U_L)$ (equal to $\frac{1}{2}U_0$ for the step flow) may be used to scale the frequency axis. If this scaling is done, the higher frequency crest of the coherence function remains centred around a relatively constant value near 0.25 for the first three downstream positions. This value is closely comparable to non-dimensional frequency values of large-scale structure measured by Browand & Troutt (1983) for mixing layers over a wide range of λ. This result again indicates the similarity of the early development of the step flow to the plane mixing layer.

The last two coherence plots show the change in the function for the region measured downstream of reattachment. At $x/H = 8$ the coherence at very low frequencies has decreased. However, the maximum value is still near the levels observed at $x/H = 6$. The final downstream plot from $x/H = 16$ demonstrates an important finding. The level of maximum coherence amplitude (approximately 60%) has decreased somewhat from $x/H = 8$; however, there is hardly any noticeable shift to lower-frequency content as observed prior to reattachment.

The results from the last two plots imply that spanwise structures persist far downstream of reattachment; their local organization being slowly eroded by viscous effects from the bounding surface. Also, pairing interactions between structures appear to be strongly inhibited by the close proximity of the solid surface since little change in frequency content is observed in this region. It should also be noted that the observed gradual decrease in coherence for this separation $\Delta z/H = 0.5$ is also in agreement with the spanwise correlation measurements present earlier.

Visualizations of the instantaneous spanwise structures are shown in figure 12. These plots were produced using the simultaneous time signals from ten hot wires aligned in the spanwise dimension. For plotting purposes additional points along the span were obtained by interpolating between hot-wire locations. The dark areas on the figures depict times during which the velocity traces are equal or above the mean; the light areas indicate times when velocities are below the mean. The figures shown here were obtained at $x/H = 6$, the downstream location of highest spanwise correlation. Figure 12(*a*) uses a timescale on the vertical axis which gives an approximately real physical view of the structures by equating downstream convection

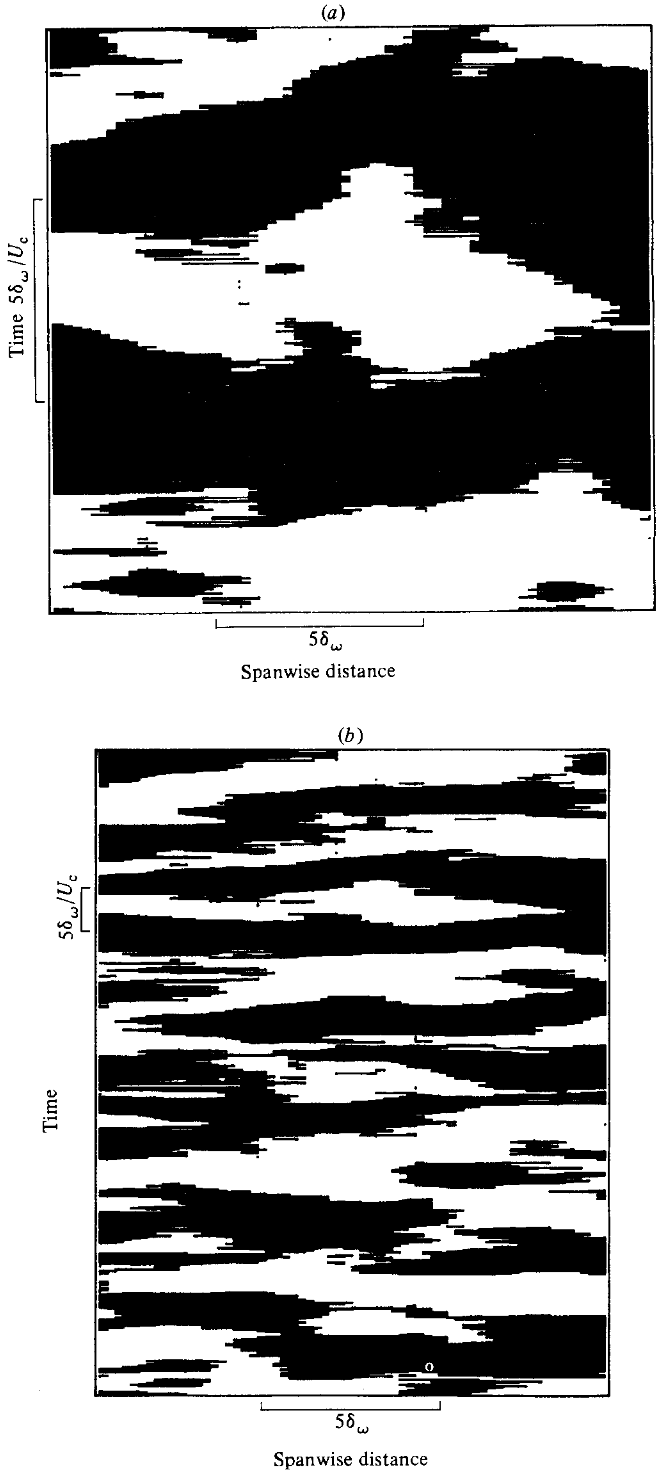

FIGURE 12. Instantaneous conditional velocity patterns from $x/H = 6.0$. Dark areas indicate values of fluctuating velocity equal to or above the mean velocity. Light areas indicate fluctuating velocities below mean. (a) Short time sequence indicating approximate physical lengthscales. (b) Extended time sequence demonstrating typical structure character.

distance with spanwise distance (the measured convection velocity of the structures in this flow obtained from downstream correlation measurements is 0.58 U_0).

Figure 12(*b*) shows a longer time period to give a more overall picture of the structure character. The spanwise structures pictured in these plots are very reminiscent of the asymptotic mixing-layer structures reported by Browand & Troutt (1980*a*) and by Browand & Troutt (1983) for similar visualizations. Although the structures are not perfectly aligned in the spanwise direction, they are definitely not the highly three-dimensional eddies postulated from conventional statistical arguments.

Browand & Troutt (1980*a*) hypothesized that pairing interactions between neighbouring vortices create spanwise distortions. The mean shear, however, works to reorganize their two-dimensionality such that asymptotic structures with non-dimensional spanwise-correlation scales, independent of downstream position, are produced. The results presented here including the correlation measurements, coherence-function analyses, and finally these visualizations, indicate that similar vortex processes are occurring in the step flow prior to reattachment.

4. Conclusions

The measurements presented strongly support the importance of large-scale organized structures in reattaching separated flow fields. Prior to the reattachment region in this step flow, the organized structures appear to behave much like the plane mixing-layer vortex structures observed in numerous recent investigations. Pairing interactions between structures occur and spanwise correlation scales comparable to mixing-layer scales are obtained. These general conclusions have also been forwarded by Eaton & Johnston (1981). In addition, direct support for the presence of coherent vortices in reattaching separated flows has been obtained in a recent visualization study of the flow over a delta wing by Gal-el-Hak, Blackwelder & Ho (1983). Their results clearly depict the existence of coherent vortices and pairing interactions in the separation region near the leading edge of the wing.

In the mean-flow reattachment region, local minimums in cross-correlation values for constant spanwise displacement are measured. Downstream of this region, the correlation values for small spanwise displacement ($\Delta z/H = 0.5$) increase and then gradually decrease with downstream position. Downstream of reattachment, the correlation values for larger ($\Delta z/H = 1.5$) displacement show very gradual increases with downstream position.

A coherence-function analysis between closely separated spanwise sensors indicates that organized large-scale structures persist far downstream of the reattachment region. The absence of shift in frequency content for the coherence function in this region indicates that pairing interactions are strongly inhibited in this region. The lack of a strong, low-frequency shift in the coherence function between $x/H = 6$ and $x/H = 16$ also sheds doubt on the hypothesis by previous investigators (see Eaton & Johnston 1981) that large-scale structures might alternately sweep upstream or downstream at reattachment.

The apparent inhibition of vortex-pairing activity in the region downstream of reattachment may also explain the slight increases in correlation values for $\Delta z/H = 1.5$ mentioned earlier. Since pairing interactions decrease spanwise correlations on a large scale, the absence of these interactions might be expected to increase the global two-dimensionality of the vortices. For smaller separations ($\Delta z/H = 0.5$), viscous effects caused by the bounding surface may be the dominant influence.

These results may be used to explain some of the interesting time-averaged behaviour of the two-dimensional step flow. One important feature of this flow is the very slow adjustment of the reattached flow to a self-preserving boundary-layer mean-velocity profile. The departure of the mean-velocity profiles in this region from classic turbulent boundary-layer profiles takes the form of a retarded flow in the outer portion of the inertial sublayer. Chandrsuda & Bradshaw (1981) attributed this 'dip' in velocity in this region to the presence of an abnormally large lengthscale. Our measurements lead us to believe this large lengthscale is directly associated with the very slowly eroding large-scale organized vortices created in the separated-flow region.

The second important time-average feature of this flow which may be interpreted from an organized structure viewpoint concerns the abrupt fall off in cross-stream Reynolds stresses and turbulence energy observed near the reattachment region by numerous investigators. Our measurements imply that this region coincides with an apparent halt in vortex-pairing activity. Browand & Weidman (1976) and, more recently, Browand & Ho (1983) have pointed out that vortex pairing is an important Reynolds-stress generation mechanism in plane mixing layers. Oster & Wygnanski (1982) have even measured negative values of cross-stream Reynolds stresses in a plane mixing layer under forcing conditions which inhibit pairings. Our results indicate that the close proximity of the bounding surface in the reattached flow also inhibits pairings, and thus a resulting sharp decline in Reynolds stress and turbulence energy follows.

At present, our results on the previous point are somewhat implicit since we have not yet measured Reynolds-stress levels in our flow field. We are now beginning a measurement programme that will concentrate on Reynolds-stress production in our flow. This study will involve instantaneous and conditionally sampled stress quantities as well as conventional long-time-average analyses. We hope these measurements will more explicitly detail the importance of vortex interactions in this flow.

The authors thank the National Science Foundation (Grant CME81-05945) and the Washington State University Office of Grant and Research Development for their financial support. The authors would also like to acknowledge the invaluable assistance of Bob Lentz and Mike Shook with regard to the development of the digital data-acquisition system used in this research and of Pat Martin in preparing the manuscript.

REFERENCES

Browand, F. K. & Ho, C. M. 1983 The mixing layer: an example of quasi two-dimensional turbulence. *J. Méc. Théor. Appl., Special Suppl.* pp. 99–120.

Browand, F. K. & Latigo, B. O. 1979 Growth of the two-dimensional mixing layer from a turbulent and nonturbulent boundary layer. *Phys. Fluids* **92**, 1011–1019.

Browand, F. K. & Troutt, T. R. 1980*a* A note on spanwise structure in the two-dimensional mixing layer. *J. Fluid Mech.* **97**, 771–781.

Browand, F. K. & Troutt, T. R. 1980*b* The geometry of the large scale structure of the turbulent mixing layer. In *Proc. 15th Intl Congr. Theor. Appl. Mech., Univ. Toronto.*

Browand, F. K. & Troutt, T. R. 1983 The turbulent mixing layer: geometry of large vortices. Submitted to *J. Fluid Mech.*

Browand F. K. & Weidman, P. D. 1976 Large scales in the developing mixing layer. *J. Fluid Mech.* **76**, 127–144.

Brown, G. L. & Roshko, A. 1974 On density effects and large structure in turbulent mixing layers. *J. Fluid Mech.* **64**, 775–816.

CHANDRSUDA, C. & BRADSHAW, P. 1981 Turbulence structure of a reattaching mixing layer. *J. Fluid Mech.* **110**, 171–194.

EATON, J. K. & JOHNSTON, J. P. 1981 A review of research on subsonic turbulent flow reattachment. *AIAA J.* **19**, 1093–1100.

GAD-EL-HAK, M., BLACKWELDER, R. F. & HO, C. M. 1983 Coherent structures in steady and unsteady motions of a delta wing. *Bull. Am. Phys. Soc., Ser. II* **28**, 1397.

KLEBANOFF, P. S. 1955 Characteristics of turbulence in a boundary layer with zero pressure gradient. *NACA Rep.* 1247.

KUEHN, D. M. 1980 Effects of adverse pressure gradient on the incompressible reattaching flow over a rearward-facing step. *AIAA J. Tech. Note* **18**, 3.

OSTER, D. & WYGNANSKI, I. 1982 The forced mixing layer between parallel streams. *J. Fluid Mech.* **123**, 91–130.

PERRY, A. E. & CHANG, M. S. 1982 On the mechanism of wall turbulence. *J. Fluid Mech.* **119**, 173–217.

WINANT, C. D. & BROWAND, F. K. 1974 Vortex pairing: the mechanism of turbulent mixing layer growth at moderate Reynolds number. *J. Fluid Mech.* **63**, 327–361.